Applied Energy 238 (2019) 760–774

Contents lists available at ScienceDirect

Applied Energy

journal homepage: www.elsevier.com/locate/apenergy

Parametric modeling of life cycle greenhouse gas emissions from photovoltaic power

Ian Miller[a,b], Emre Gençer[a,*], Hilary S. Vogelbaum[a,c], Patrick R. Brown[a], Sarah Torkamani[d], Francis M. O'Sullivan[a,*]

[a] MIT Energy Initiative, Massachusetts Institute of Technology, 77 Massachusetts Avenue, Cambridge, MA 02139, United States
[b] Department of Chemical Engineering, Massachusetts Institute of Technology, 77 Massachusetts Avenue, Cambridge, MA 02139, United States
[c] Department of Materials Science and Engineering, Massachusetts Institute of Technology, 77 Massachusetts Avenue, Cambridge, MA 02139, United States
[d] ExxonMobil Research and Engineering Company, Annandale, NJ 08801, United States

HIGHLIGHTS

- Ignoring temperature underestimates solar power emissions by > 10% in warm regions.
- Solar tracking changes power emissions by ± 12%, dependent on cell type & location.
- Chinese solar module production emits ~25% more greenhouse gases than European.
- Emissions of most carbon intense solar power < 25% emissions of natural gas power.
- Photovoltaic performance modeling improves life cycle analysis of solar power.

ARTICLE INFO

Keywords:
Photovoltaic (PV) power
Life cycle assessment (LCA)
Greenhouse gas (GHG) emission
Solar tracking
Inverter loading
Degradation

ABSTRACT

From 2007 to 2017, global installed solar photovoltaic power capacity grew by a factor of 50. Practices that were minor, including solar tracking, inverter overloading, and Chinese module manufacturing, became mainstream. Countries including the US and India installed large amounts of solar in warm regions with mean temperatures above 20 °C. The impacts of these developments on greenhouse gas emissions from photovoltaic power have not been analyzed by life cycle assessment in depth. This study helps to fill that gap. A modeling tool is built that integrates photovoltaic life cycle inventories, background emission factors, known physical correlations, and modern photovoltaic performance modeling, including temperature-dependent performance ratios. Using this tool, four novel findings are produced on life cycle greenhouse gas emissions from photovoltaic power, referred to here as carbon intensity. Firstly, reversible temperature effects on modules raise the carbon intensity of silicon photovoltaic power installed in warm regions, including by 10% in the southwestern US and 13% in western India. All temperature effects raise silicon photovoltaic carbon intensity by ~23% in southern India (from 35 to 43 gCO_2e/kWh). Secondly, emission impacts of tracking, relative to stationary mounting, depend on installation location and module type. For multi-crystalline silicon and cadmium telluride modules, respectively, adding tracking changes carbon intensity by −11% and −3% in the southwestern US, and by −4% and +5% in eastern Australia. This dependence on location and module type, and the novel result that tracking can increase emissions intensity, is explained by interactions between tracking energy gain, tracker production emissions, and module production emissions. Thirdly, Chinese manufacturing of multi-crystalline silicon modules emits ~25% more greenhouse gases than European manufacturing, due not only to higher carbon intensity of upstream electricity, as previously reported, but also to more electricity and fuel input per module produced. Fourthly, inverter overloading as practiced slightly diminishes photovoltaic carbon intensity, by less than 2 gCO_2e/kWh. Finally, mainstream photovoltaic power in all its forms has significantly lower life cycle greenhouse gas emissions than fossil power.

* Corresponding authors.
E-mail addresses: egencer@mit.edu (E. Gençer), frankie@mit.edu (F.M. O'Sullivan).

https://doi.org/10.1016/j.apenergy.2019.01.012
Received 27 July 2018; Received in revised form 29 November 2018; Accepted 1 January 2019
Available online 25 January 2019

Nomenclature

Abbreviations

AC	alternating current
BOS	balance of system
CCNG	combined cycle natural gas
CdTe	cadmium telluride
CIGS	copper indium gallium selenide
EOL	end of life
gCO_2e	grams CO_2 equivalent
GHG	greenhouse gas
GHI	global horizontal irradiance
ILR	inverter loading ratio
LCA	life cycle assessment
LCI	life cycle inventory
LID	light-induced degradation
mc-Si	multi-crystalline silicon
MG-Si	metallurgical grade silicon
PR	performance ratio
PV	photovoltaic
sc-Si	single-crystalline silicon
SCPC	supercritical pulverized coal
SG-Si	solar grade silicon
TEG	tracking energy gain
TMY	typical meteorological year

Symbols

A	module area (m^2)
A_{op}	module area at operating installation (m^2)
a	amount (e.g., kg-iron, m^3-acetone)
$c_{AC,inv}$	rated AC inverter capacity (kW)
c_{DC}	rated DC capacity (kW)
CF	capacity factor
$\bar{CF}$	lifetime average capacity factor
CF_{fixed}	capacity factor given fixed orientation
CF_{PVW}	capacity factor from PVWatts
CF_{snow}	capacity factor, adjusted for snow losses
CF_{track}	capacity factor given tracking
CF_{yr1}	capacity factor in first operating year
CI	carbon intensity (gCO_2e/kWh)
d	degradation rate (fraction/yr)
E_{AC}	AC electricity produced (kWh)
EF	emission factor (gCO_2e/[amount])
e	emissions (gCO_2e)
η_{STC}	rated module efficiency
f	fraction
$f_{loss,op,1yr}$	fraction of modules replaced per year
f_{sh}	fraction of irradiance blocked by shade
f_{snow}	fraction of irradiance blocked by snow
$\bar{I}$	average solar irradiance (kW/m^2 or $kWh/yr/m^2$)
I_{STC}	irradiance used for rating modules, 1 kW/m^2
m_{mount}	mass of mounting system (kg)
P	power (kW)
$\bar{P}_{AC}$	lifetime average AC power (kW)
P_{track}	power consumed by tracker (kW)
t	lifetime (yr)

1. Introduction

The driving forces for this study are (1) the lack of life cycle assessments (LCAs) analyzing several major developments in photovoltaic (PV) power production, and (2) the need for more detailed PV performance models to analyze these developments and their environmental impacts. This paper is the first LCA to analyze inverter overloading; the first to analyze solar tracking's emissions impact over multiple locations and to provide equations that explain that impact; and the first to analyze temperature impacts on emissions from PV power.

1.1. Background

The electric power sector produces 40% of global greenhouse gas emissions [1]. To limit human-caused global warming to 2 °C, the IEA projects that power sector emissions must drop 90% by 2050, from 13 to 1.4 gigatons of carbon dioxide per year [1]. To help achieve this decline, many governments have increased their support for low-carbon power sources. Due to this support and large cost reductions [2], global installed PV power capacity grew by a factor of 50 from 2007 to 2017 [3]. PV power production has grown from 0.03% of global electricity in 2006 to 1.3% in 2016 [4], and is projected to reach 5–15% by 2040 [5,6]. In some regions, photovoltaics already produce this level of power, including Germany (7% in 2016) [7] and California (10% in 2016) [8]. The most widely deployed PV cell types are multi-crystalline silicon (mc-Si), single-crystalline silicon (sc-Si), and cadmium telluride (CdTe), with market shares of 70%, 24%, and 4%, respectively, of new PV installed in 2016 [7].

While PV power's operating greenhouse gas (GHG) emissions are negligible compared to those of fossil power, its upstream emissions are not. GHG emissions from the entire life cycle of PV power production have been estimated at 76, 53, and 27 g of CO_2 equivalent per kilowatthour of AC electricity generated (gCO_2e/kWh) for sc-Si, mc-Si, and CdTe PV, respectively, installed in northern Europe circa 2015, and at 33, 22, and 13 gCO_2e/kWh for PV installed in the US southwest circa 2015 [9]. For context, representative GHG emissions from large onshore wind, combined cycle natural gas, and supercritical pulverized coal power are approximately 12 [10], 488, and 965 gCO_2e/kWh [11], respectively. This paper refers to life cycle GHG emissions per unit of AC electricity generated (gCO_2e/kWh) as carbon intensity.

The leading method for estimating carbon intensity is life cycle assessment (LCA). As outlined by ISO standards 14040 and 14044 [12], LCA quantifies a product's environmental impacts through input-output accounting of cradle-to-grave or cradle-to-gate processes. Since 2007, over 50 studies have conducted LCA of PV power. Hou et al. [13] found that grid-connected sc-Si PV in China emitted 60–87 gCO_2e/kWh, dependent on installation conditions, and that module manufacturing accounted for over 84% of life cycle emissions from PV power. Akinyele et al. [14] analyzed emissions of power from residential systems, installed at 6 locations spanning Nigeria, and found that carbon intensity ranged from 37 to 72 gCO_2e/kWh. The study assumed constant performance ratio between regions. Kabakian et al. [15] also analyzed a small residential system, in this case in Lebanon, and found that the addition of batteries increased the carbon intensity of power reaching the user by a small amount, from 39 to 40 gCO_2e/kWh. Yu et al. [16] compared different production methods for solar-grade silicon, and found that PV power from mc-Si produced via an alternative metallurgical route, compared to the mainstream modified Siemens process, reduced total environmental impact (dimensionless units) by over 5%. In summary, the PV LCA literature has found that the top drivers of PV carbon intensity are upstream electricity source, cell type, module efficiency, irradiance at installation site, and system lifetime [17,18]. Peng et al. [18] provided a detailed literature review of PV LCA and underlined several gaps in the field, including the treatment of cell temperature and module orientation. IEA reports from 2008, 2011, and 2016 [19] provided methodology guidelines for PV LCA, and

recommended that practitioners quantify emissions on a per AC kilowatthour basis, thus facilitating comparison to other power sources.

1.2. Motivation

Since 2008, PV power production has changed significantly. Some of these changes have not been analyzed by LCA at all or in depth. This paper aims to help fill that gap. In particular, we analyze the impact on PV carbon intensity of several practices that were minor in 2008 and are mainstream now, namely, inverter overloading, solar tracking, and Chinese mc-Si module production. In addition, we analyze the emissions impact of geographic temperature variation. Analyzing these impacts requires more detailed models of PV performance than PV LCAs have typically employed, including temperature-dependent performance ratios. This paper incorporates PV performance modelling via the use of capacity factors calculated with PVWatts, a software tool from the US National Renewable Energy Laboratory (NREL) [20].

The inverter loading ratio (ILR) of a PV system is the ratio of rated DC module capacity to rated AC inverter capacity. Inverter overloading is the practice of installing more module capacity than inverter capacity, thus yielding an ILR above 1. In the US, the mean ILR of new large-scale PV projects (AC capacity > 1 MW) rose from 1.09 in 2009 to 1.25 in 2016, while the share of new projects with ILRs of 1.4 or more grew from 0% to 23% (112 of 478 new projects in 2016) [21]. While inverter overloading has become the norm for PV power, its impact on PV carbon intensity has not been analyzed in the LCA literature.

As solar tracking becomes more common, estimating its emissions impacts becomes more relevant. Utility-scale PV (AC capacity > 5 MW) increasingly employs tracking, including 53% of cumulative and 70% of new capacity in the US in 2016 [21]. In the US from 2008 to 2014, only 19% of new utility-scale CdTe projects had tracking (16 of 86 projects); in 2015 and 2016, the number was 56% (44 of 79 projects), including locations outside the exceptionally sunny US southwest, such as Colorado, Tennessee, and Georgia [21]. Several LCAs analyzed the emissions impact of solar tracking, but with limited geographic scope and tracking set-ups that are not (and do not claim to be) representative of industry practice [22–24]. Bayod-Rújula [22] analyzed a 2-axis tracking system in Spain. Desideri et al. [24] and Beylot et al. [23] analyzed hypothetical 1-axis tracking systems with 30° tilt in Italy and an unspecified location, respectively. In contrast, the industry norm for PV tracking is horizontal 1-axis tracking; in the US in 2016, 97% of utility-scale tracking PV projects used horizontal 1-axis tracking (255 of 263 projects) [25].

Two PV LCAs analyzed industry-representative tracking set-ups. Leccisi et al. [9] found that horizontal 1-axis tracking reduced carbon intensity by 11% and 1% for mc-Si and CdTe PV, respectively, given installation in the US southwest. The study concluded that “one-axis tracking installations can improve the environmental profile of PV systems by approximately 10% for most impact metrics.” Similarly, Sinha et al. [26] estimated that tracking reduced the carbon intensity of CdTe PV by 3% in the US southwest, and concluded that “tracking systems…provide an eco-efficient strategy for improving the sustainability of PV systems.“ However, neither study calculated tracking's impact outside the US southwest. This paper builds on these studies by calculating tracking's impact on PV carbon intensity over a range of locations, and by explaining that impact.

The impact of temperature variation is relevant when estimating PV emissions intensity in any location, and especially relevant when comparing intensities across different climates. Several LCAs analyzed PV across regions with large mean temperature differences (> 15 °C) [9,27,28]. A common approximation in these studies is temperature-independent performance ratio (PR). Perpiñan et al. [27] assumed constant cell temperature between central France and the central Sahara desert. Nian [28] assumed constant performance ratio across northern Europe, the Middle East, Japan, Australia, the northern US, and Singapore. Leccisi et al. [9] assumed constant performance ratio between northern Europe and the US southwest. The approximation of constant PR is not problematic in most prior PV LCAs, but it can be problematic for inter-regional emissions comparisons. It would be inaccurate to ignore regional irradiance differences and their impacts on module power output; similarly, it is inaccurate to ignore regional temperature differences and their impacts on module power output. High temperatures reduce module operating efficiency and thus PR, both reversibly (via voltage decrease) [29] and irreversibly (via corrosion, discoloration, micro-cracking from thermal cycling, and other mechanisms) [30]. A typical silicon module's efficiency reversibly declines by ~0.47% (relative) for every 1 °C increase in cell temperature, a phenomenon that is well understood and based on statistical analysis of performance data from over 11,000 modules [20]. Irreversible efficiency reduction (degradation) from high temperatures is less well characterized but can be a similar order of magnitude over a typical system lifetime [31]. Whether reversible or irreversible, efficiency reductions decrease power output, and thereby increase the emissions intensity of PV power ($g_{emissions}$/kWh). This study estimates the magnitude of such increases.

2. Methodology

We developed a PV LCA modeling tool following the ISO 14040 and 14044 standards [12] and the IEA PV LCA guidelines [19]. Table 1 summarizes how our analysis corresponds to these guidelines. In addition to elaborating several items in Table 1, this section describes how the modeling tool operates. We refer to the tool as SoLCAT (Solar Life Cycle Assessment Tool). To estimate attributional life cycle GHG emissions from PV power under diverse conditions, SoLCAT integrates four main elements: published PV life cycle inventories (LCIs), background emission factors from the Ecoinvent database [32], known physical correlations (e.g., the relation between rated module efficiency and capacity), and capacity factors from PVWatts.

2.1. LCA goals, system boundary, and functional unit

Our primary goal is estimating how the life cycle GHG emissions of PV power are impacted by inverter overloading, solar tracking, geographic temperature variation, and Chinese mc-Si module production. Our system is electricity production by PV. Electricity production can be considered a black box that consumes resources and produces electricity and emissions. The system's primary function is producing electricity, and thus the functional unit is AC electricity supplied to the grid. In addition to electricity, the other system output analyzed is GHG emissions. These two system outputs are combined into our central metric: GHGs emitted per AC electricity generated (gCO_2e/kWh), referred to as carbon intensity in this paper.

PV electricity production can be elaborated as shown in Figs. 1 and 2. Commercial thin film module production is relatively less complex and more vertically integrated [34,35], and is not further segmented beyond Fig. 1. Crystalline silicon module production is further elaborated here, as shown in Fig. 2.

LCA refers to the explicit stages in Figs. 1 and 2 as the “foreground” and their implied component processes as the “background”. It should be emphasized that background processes are within the system and include: production of chemicals used in silicon processing, construction and operation of module manufacturing infrastructure, and raw material extraction processes (e.g., iron ore acquisition, aluminum ore acquisition) that “pull” resources from nature, across the system boundary, and into the electricity production system. In this analysis, transport is treated as a background process that contributes to multiple foreground stages. For example, chemicals are transported to the site of

Table 1
Summary of correspondence of this study to IEA PV LCA methodology guidelines [19]. (Note: Because this work includes multiple case studies, some items lack single values. In such cases the table reads "variable" and their values are specified in individual cases in Section 3.)

Item recommended by IEA guidelines	Value in this analysis
Goal of analysis	To estimate how PV power's life cycle GHG emissions are impacted by inverter overloading, solar tracking, geographic temperature variation, and Chinese mc-Si module production
LCA approach	Process-based LCA, also called attributional LCA
LCA software tool	Tool built and presented here (SoLCAT). See methodology
LCI databases used	Ecoinvent database V3 [32]
Impact indicator method used	IPCC 2013 GWP 100a
Life cycle stages included	Raw material acquisition through power plant operation. See life cycle diagrams in Figs. 1 and 2. EOL of power plant is not included in emissions calculations due to lack of data
PV cell type	Variable. Analyzed values include: sc-Si, mc-Si, CdTe, and CIGS
Installation type	Variable. Analyzed values include: utility-scale fixed-tilt, utility-scale with horizontal 1-axis tracking, rooftop optimal tilt, rooftop "typical" tilt
Efficiency, STC rated (%)	Variable
Degradation rate (%/yr)	Variable
Lifetime of modules	Variable. Consistent with LCI data sources [35,37], module losses are assumed at 1% during installation, and 2% over 30 years of operation (0.067% per year) due to module damages beyond linear degradation
Lifetime of BOS	For inverters, 15 years. For mounting, module lifetime
Location of installation	Variable
Annual irradiance (kWh/m^2/yr)	Variable. In this analysis, incident irradiance depends on location, installation type (via orientation), and other model inputs. See Section 2.4 and supplement on performance modeling
Module orientation	Variable and determined by installation type. Possible values include: - optimal orientation (equator facing, and irradiance-maximizing tilt, which can deviate from latitude tilt, e.g. by −9° in Berlin). This orientation is employed by the installation options "utility-scale fixed-tilt" and "rooftop optimal tilt" - time-varying orientation, i.e. 1-axis east-west tracking with horizontal tilt & 45° rotation limit - "typical" rooftop orientation (28° tilt and ± 45° deviation from equator facing)[a] [33]
Annual electricity production	Variable. Value depends on location, orientation, and other model inputs. See Section 2.4 and supplement 1 on performance modeling
Performance ratio (PR)	Variable. PR is not assumed constant across locations or time, due to temperature differences, snow, and other effects. This is an important aspect of this work
Region of production modeled	Variable. Analyzed values include: China (for mc-Si), Europe (for mc-Si and sc-Si), Malaysia (for CdTe), and Japan (for CIGS). Carbon intensity of upstream electricity, a model input, influences this item because certain carbon intensities are characteristic of certain regions
Upstream electricity source	Variable, via variation of model inputs, namely, carbon intensities of upstream electricity used to make module & BOS

[a] "Typical" is in quotes because this tilt and azimuth are based on those found to be most common among PV-suitable rooftops in an NREL survey of ~23% of buildings in the continental US [33]. Typical orientations may differ by region. SW and SE azimuths occur at roughly equal levels in the buildings surveyed, and thus the capacity factor utilized by SoLCAT for a "typical" rooftop orientation in a location is the average of two capacity factors, one for 28° tilt and −45° deviation from equator-facing, and one for 28° tilt and +45° deviation from equator-facing. These capacity factor pairs differ minimally, by at most 2% at high latitudes (e.g. London), 1% at medium latitudes (e.g. Boston), and 0% at low latitudes (e.g. Singapore).

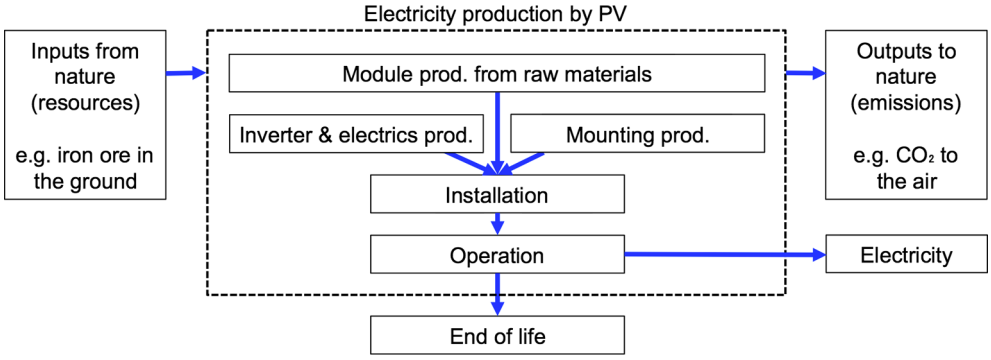

Fig. 1. Life cycle stages of PV electricity production.

silicon processing, and solar glass is transported to the site of module production. In other words, like materials and energy, transport is treated as an input to each stage. To be consistent, when the output of foreground process A is input to foreground process B, transport of the item is considered part of process B. Given multiple valid ways of segmenting life cycle and inputs, and the possibility that different segmentations provide different insights, SoLCAT reports emissions breakdowns both by life cycle stage (cell production emissions, installation emissions, etc.) and by foreground input category (electricity emissions, transport emissions, etc.). Processes not included in our system include: electricity transmission from generation site to end use, displacement of competing power sources, and growth of carbon absorbing biomass underneath PV modules, which growth can be reduced by up to ~75% by module shading in temperate climates [36].

2.2. Data sources

A list quantifying inputs and outputs of a stage is called a life cycle inventory (LCI). Our primary sources for PV foreground LCIs are the IEA's 2015 Report "Life Cycle Inventories & Life Cycle Assessments of PV Systems" [37] and the ESU's 2012 Report "Life Cycle Inventories of Photovoltaics" [35]. These sources aggregate large numbers of LCIs and explicitly aim to represent production typical of the PV industry. For each stage of Chinese mc-Si module production, the IEA report [37] provides a "mainstream production" LCI and a "best technology" LCI. The mainstream LCIs are utilized in our model, while the best technology LCIs are used in a sensitivity analysis. Other sources for foreground LCIs are the Ecoinvent Database V3 [32] for an LCI of silica sand acquisition, and Sinha et al. [26] for an LCI of a horizontal 1-axis

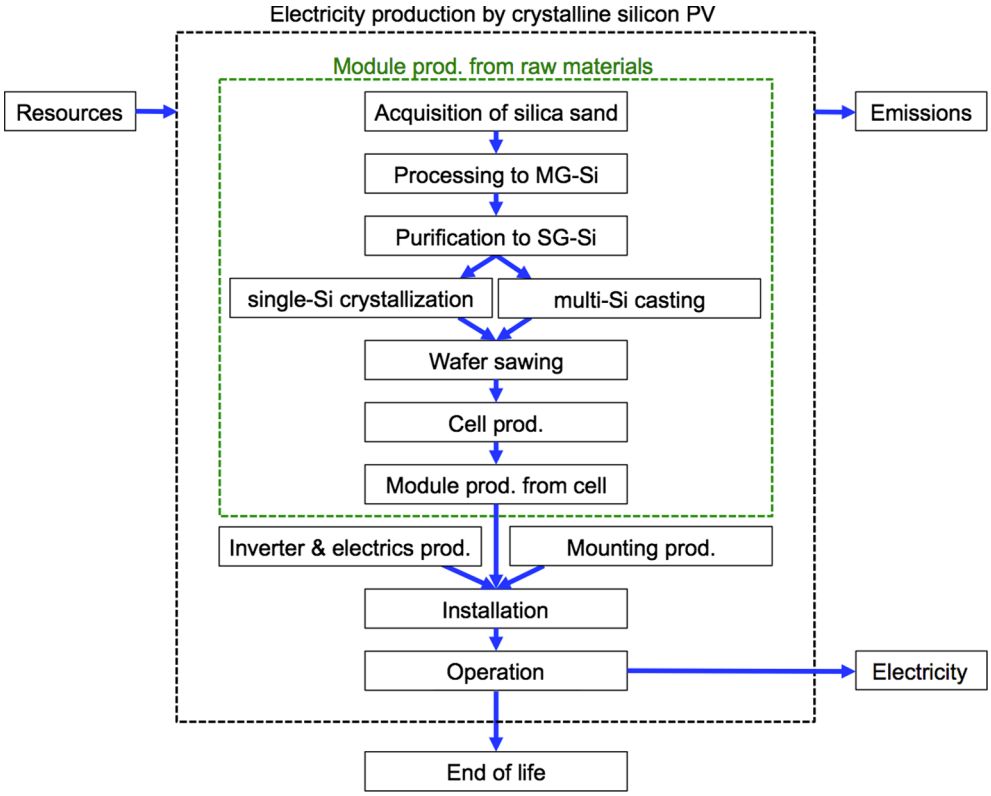

Fig. 2. Life cycle stages of electricity production by crystalline silicon PV.

tracking system.

To calculate life cycle GHG emissions from PV electricity, data is needed not just on foreground LCIs but also on emission factors for hundreds of background processes. Our primary source for this data is the Ecoinvent V3 database [32]. The impact assessment method used by Ecoinvent V3 and thus by our model to calculate emission factors in units of CO_2 equivalent is IPCC 2013 GWP 100a [38].

The PV LCI sources used here are the most comprehensive available, but have two features which potentially constrain the applicability of our model. First, the IEA LCIs [37] utilize industry data collected before 2015. For the Chinese mc-Si LCIs, approximately half the data are from 2014 and half from 2011. The 2014 data include electricity inputs to all life stages, and a majority of all inputs to casting, wafer production, and solar-grade Si production. The 2011 data are mainly material inputs to metallurgical-grade (MG) Si production and module assembly. MG-Si production is a carbothermic reduction process that is technologically mature and has been used by non-PV industries including electronics for over 50 years. It emits little (< 5%) of silicon PV's life cycle carbon, and a majority of this small share comes from using electricity, for which our model uses more recent data. In total, the 2014 Chinese mc-Si data accounts for ~75% of life cycle carbon emissions.[1] The IEA LCIs for European mc-Si, sc-Si, and thin film production use older data, published in 2014 by de Wild-Scholten [39], but collected from industry in 2011. The pre-2015 age of all foreground LCI data is mitigated by the use of more recent data on background inputs (via Ecoinvent) and electricity sources (via annual IEA reports on electricity emissions by country [40]). Additionally, average wafer thickness and silicon usage per module capacity have been approximately constant since 2008 and 2012 [7], respectively, suggesting that 2011 and 2014 foreground data on wafer and module production remain applicable.

Second, the referenced LCIs do not provide data on end of life (EOL). Limited reliable data exists regarding PV EOL, because the large majority of PV installed has not reached its end of life. In the absence of data, our model does not account for emissions from EOL processes. Wind power LCAs, which face a similar lack of EOL data, sometimes approximate end-of-life as the reverse of installation and thus assume equivalent emissions [10].

2.3. Model structure

SoLCAT uses foreground LCIs and background emissions factors in several ways to estimate the carbon intensity of PV power. Fig. 3 gives an overview of SoLCAT's operation and utilization of data sources. Capacity refers to rated DC power capacity, unless otherwise indicated.

SoLCAT converts amounts (a) to GHG emissions per capacity using three general equations, shown below with indented examples after each equation:

$$e_{total} = \sum_i e_{stage i} \quad (1)$$

$$e_{total,mc-Si} = e_{Si-sand\ \ acquistion} + e_{MG-Si\ \ processing} \cdots + e_{cell\ \ prod.} \cdots + e_{installation} + e_{operation}$$

$$e_{stage\ \ i} = \sum_j e_{input\ \ j\ \ to\ \ stage\ \ i} - \sum_k^{stages\ \ before\ \ i} e_{stage\ \ k} \quad (2)$$

$$e_{MG-Si\ \ process.} = (e_{charcoal\ \ input\ \ to\ \ MG-Si\ \ process.} + e_{Si-sand\ \ input\ \ to\ \ MG-Si\ \ process.} + \ldots) - e_{Si-sand\ \ acq.}$$

$$e_{input\ \ j\ \ to\ \ stage\ \ i} = a_{input\ \ j\ \ to\ \ stage\ \ i}\ EF_j \quad (3)$$

$$e_{chromium\ \ steel\ \ input\ \ to\ \ mounting\ \ prod.} = a_{chromium\ \ steel\ \ input\ \ to\ \ mounting\ \ prod.}\ EF_{chromium\ \ steel}$$

where e is emissions (gCO_2e), a is amount (e.g., kg-iron, m^3-acetone, etc.), and EF is emission factor (e.g., gCO_2e/kg-iron, gCO_2e/m^3-

[1] The exact share depends on assumed electricity sources and other parameters, as elaborated in Section 2.3.

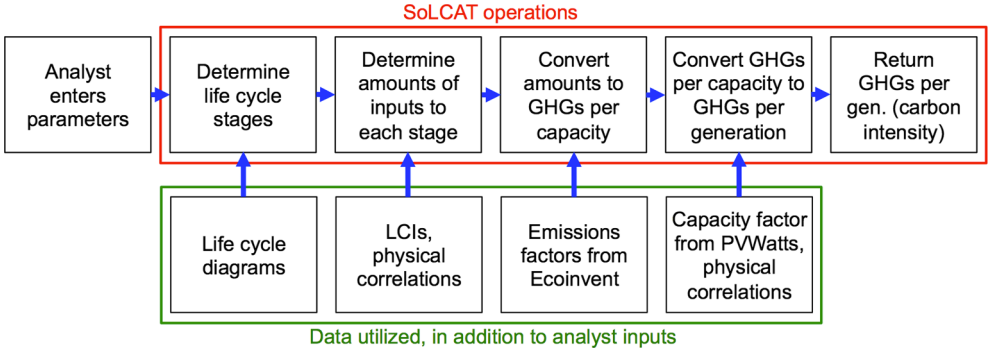

Fig. 3. Flowchart of SoLCAT operations and utilization of data sources. Capacity is rated DC capacity. Generation is AC electricity generation.

Table 2
Model input variables and utilization by SoLCAT.

Input variable [symbol] (unit)	Selectable values	Important uses in SoLCAT	Relevant equations (red indicates input variable)
Location of installation	locations across globe	Determines location inputs to: (1) PVWatts, which determines weather data (including irradiance, temperature, wind speed, and albedo) and thus effects year-one capacity factor; and (2) NREL's System Advisor Model snow model [41], which determines snow losses	(1) See Section 2.4 and supplement on performance modeling (2) $CF_{snow} = CF_{PVW}/(1 - f_{snow})$
Cell type	sc-Si mc-Si CdTe CIGS	(1) Determines which module production LCIs are referenced and thus types and amounts of inputs to module production stages. (For mc-Si, an additional choice is made between Chinese and European production) (2) Determines cell type input to PVWatts, and thus thermal coefficient (γ) and other properties used to model performance (3) If CdTe selected, adjusts nameplate error and light-induced degradation to 0% from PVWatts c-Si-based defaults of 1% and 1.5%, respectively	(1) Eq. (3) (2) See Section 2.4 and supplement Table S.1
Installation type	utility, fixed tilt utility, 1-axis tracking rooftop, optimal tilt rooftop, typical tilt	(1) Determines BOS LCIs referenced and thus types and amounts of inputs to BOS production stages (production of mounting, inverter & electrics) (2) Determines installation type and orientation input to PVWatts, which effects incident irradiance, module temperature, and year-one capacity factor (3) Adjusts capacity factor for small tracker energy consumption based on [26]. If tracking not selected, $P_{track,perA} = 0$	(1) Eq. (3) (2) See Section 2.4 and supplement (3) $CF = \bar{CF} - \frac{P_{track}}{c_{DC}} = \bar{CF} - \frac{P_{track,perA}}{\eta_{STC} \times I_{STC}}$
Shading losses [f_{sh}] (fraction)	(continuous)	Adjusts capacity factor from PVWatts default shading to input shading	$CF_{yr1} = CF_{snow} \times (1 - f_{sh})/(1 - f_{sh,pvw})$
Lifetime [t] (yr)	(continuous)	(1) Adjusts capacity factor from year-one to lifetime average value (2) Determines PV module area replaced due to operating damages	(1) $\bar{CF} = CF_{yr1} \times (1 - d \times t/2)$ (2) $A_{loss,op} = A_{op} \times f_{loss,op,1yr} \times t$
Efficiency, STC rated [η_{STC}] (fraction)	(continuous)	(1) Determines PV module area required for installation of known DC capacity, not including installation and operating losses (2) Determines mass of mounting system	(1) $A_{op} = c_{DC}/(I_{STC} \times \eta_{STC})$ (2) $m_{mount} = m_{mountperA} \times A_{op} = m_{mountperA} \times c_{DC}/(I_{STC} \times \eta_{STC})$
Degradation rate [d] (fraction/yr)	(continuous)	Adjusts capacity factor from year-one to lifetime average value.	$\bar{CF} = CF_{yr1} \times (1 - d \times t/2)$
Inverter loading ratio [ILR] (ratio)	(continuous)	(1) Determines inverter AC capacity required for installation of known DC capacity (2) Impacts inverter efficiency and possibility of "clipping"	(1) $c_{AC,inv} = c_{DC}/ILR$ (2) See Section 2.4 and supplement Table S.3
Upstream electricity emissions: module (gCO_2/kWh)	(continuous)	Provides emission factors of electricity used in module production stages	Eq. (3)
Upstream electricity emissions: BOS (gCO_2/kWh)	(continuous)	Provides emission factors of electricity used in BOS production stages	Eq. (3)
Shipping dist. from module prod. to installation (km)	(continuous)	Determines amount of shipping input to installation stage	Eq. (3)
If mc-Si, module prod. typical of:	Europe China	Determines LCIs referenced for stages of mc-Si module production	Eq. (3)

acetone, etc.). Calculating life cycle emissions for one scenario involves several hundred variations of Eq. (3) corresponding to different stages and inputs. Amounts ($a_{inputjtostagei}$) are provided by the PV LCIs [26,35,37,39] or determined by input variables to SoLCAT. Emission factors (EF_j) are provided by Ecoinvent [32] or SoLCAT inputs. Input-provided emission factors are (1) the carbon intensity of the electricity used to produce the modules, and (2) the carbon intensity of the electricity used to produce the balance of system (BOS). Table 2 describes how SoLCAT input variables affect amounts and emission factors.

2.4. Converting GHGs per capacity into GHGs per generation (carbon intensity)

SoLCAT's last operation requires a capacity factor, or equivalently an energy yield. In estimating this factor, our methodology differs from that of prior multi-location PV LCAs [9,17,28], which treat performance ratio as temperature- and location-independent, and model AC electricity production as:

$$E_{AC} = A \times \bar{I} \times \eta_{STC} \times PR \times t \quad (4)$$

where E_{AC} is AC electricity produced (kWh), A is module area (m^2), $\bar{I}$ is average solar irradiance (kW/m^2 or kWh/yr/m^2), η_{STC} is rated module efficiency, PR is performance ratio, and t is system lifetime (yr). Eq. (4) is not used here because it limits what can be analyzed. Instead, our model utilizes capacity factor estimates from PVWatts [20]. PVWatts outputs year-one DC capacity factor based on inputs of: location, installation type, orientation, cell type, inverter loading ratio, rated inverter efficiency, ground coverage ratio, and system losses. To elaborate its role in our model and to underline important differences from Eq. (4), an outline of PVWatts' performance model is provided in the supplement.

As shown in Table 2, our model adjusts capacity factors from PVWatts to account for shading, snow, light-induced degradation (LID), non-LID degradation (commonly called "degradation"), and tracker energy consumption, to calculate a lifetime average capacity factor (CF). Finally, carbon intensity is calculated as:

$$CI = e_{total}/(CF \times c_{DC} \times t_{hr}) \quad (5)$$

where CI is carbon intensity (gCO_2e/kWh), e_{total} is life cycle GHG emissions (gCO_2e), c_{DC} is rated DC capacity, and t_{hr} is PV system lifetime (h).

Important differences between PVWatts' performance model and Eq. (4) include: (1) module operating efficiency is modeled and temperature-dependent (see Table S.1), which enables more accurate modeling of power output across regions with significant temperature differences; (2) the interaction of location, orientation, and incident irradiance is rigorously modeled (see Table S.2), which enables more accurate modeling of solar tracking's impact on power output in different locations; and (3) Inverter efficiency is modeled and power-dependent (see Table S.3), which enables more accurate modelling of PV power output across different inverter loading ratios. The model's treatments of temperature, incident irradiance, and inverter efficiency are standard in PV performance modeling and experimentally validated, as described in the supplement and supplement references. In summary, PVWatts serves our goal of estimating PV power's carbon intensity under diverse conditions, by more accurately modeling the production of PV LCA's functional unit, AC electricity.

2.5. Tracking energy gain methodology

Analysis of solar tracking's impact on carbon intensity requires the calculation of tracking energy gain (TEG). TEG is the percent increase in PV power output that results from tracking the sun, relative to a fixed-position system, and can be estimated using PVWatts and Eqs. (S.1) and (5) as

$$TEG = (\bar{P}_{AC,track} - \bar{P}_{AC,fixed})/\bar{P}_{AC,fixed} \times 100\% \quad (6)$$

or equivalently

$$TEG = (CF_{track} - CF_{fixed})/CF_{fixed} \times 100\% \quad (7)$$

where CF_{track} is the capacity factor of a PV system with tracking, and CF_{fixed} is the capacity factor of a PV system with fixed orientation but otherwise identical features (location, modules, etc.). When discussing TEG, the details of both the tracking system (whether 1-axis or 2-axis, axis of rotation, rotation limits, etc.) and the fixed base case (tilt and azimuth) should be specified. In this paper, the fixed base case orientation is always irradiance-maximizing, with equator-facing azimuth (south in northern hemisphere, north in southern hemisphere) and near-latitude tilt.

3. Results and discussion

SoLCAT results are compared here with the most up-to-date available results on life cycle GHG emissions from mainstream PV power production, from Leccisi et al. [9]. Fig. 4 shows good agreement across cell types and irradiances. This is expected because both SoLCAT and Leccisi et al. use LCIs from the IEA's 2015 PVPS Report [37]. This agreement shows that our methodology can reproduce results obtained with the LCA software program SimaPro, which is used by Leccisi et al. Small differences may be explained by uncertainties in exact grid emission factors assumed and by use of CdTe module and BOS LCIs that are not available here.

3.1. Base cases and sensitivity analysis

This section defines base cases to compare to later results, and quantifies the sensitivity of PV carbon intensity to parameters analyzed in prior LCAs. One goal is to give a sense of the uncertainties in GHG emissions that result from uncertainties in parameters. Fig. 5 shows how carbon intensity varies by location, irradiance, and cell type. The

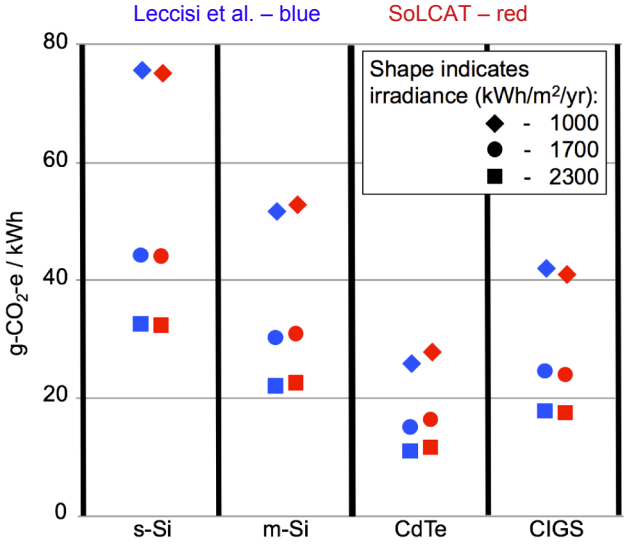

Fig. 4. Carbon intensity of PV power by cell type and irradiance. Leccisi et al. [9] results are in blue, SoLCAT results in red. To correspond to Leccisi: mounting is open-ground fixed-tilt; lifetime is 30 years; rated module efficiencies are 17%, 16%, 15.6%, and 14%, left to right; performance ratio is a constant 0.8 across irradiances and accounts for shading and degradation, among other losses; US grid in 2015 is assumed for Si & CdTe modules, and Japan's grid in 2015 for CIGS modules, with US & Japan's grid GHG emissions set to 480 & 560 gCO_2e/kWh, respectively, based on IEA electricity data [40]. Inverter loading ratio is assumed to be 1. Cell temperature and degradation are not specified by Leccisi et al., but must give a PR of 0.8 when combined with other losses. In SoLCAT, cell temperature and degradation are set at 25 °C and 0.7%/yr, while other losses are adjusted to 9.5% to give PR = 0.8.

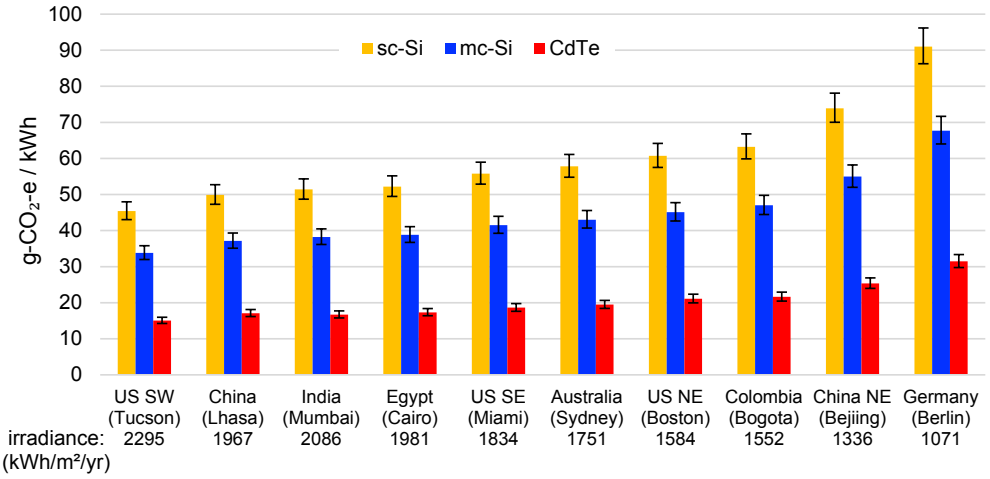

Fig. 5. Base case carbon intensities of PV power from systems installed in different locations circa 2015. Installation type is large-scale (AC capacity > 1 MW), open-ground, fixed-tilt. Orientation is irradiance-maximizing. Irradiance is lifetime-average irradiance incident on modules. Lifetime is 30 years. Mean rated module efficiencies are 17%, 16%, and 15.6% for sc-Si, mc-Si, and CdTe, respectively, corresponding to average commercial efficiencies in 2015 [7]. Mean degradation is 0.7%/yr, corresponding to IEA PV LCA guidelines [19] and to measured degradation rates [30], which do not evidence a lower rate for CdTe vs. c-Si, despite warranties suggesting otherwise. Inverter loading ratio is 1. GHG emissions of upstream electricity are 660 gCOe/kWh for module production and 510 for BOS production, corresponding to Chinese & global averages in 2015 [40]. Total non-modeled losses, enumerated in methodology, are 14% for silicon and 11% for CdTe, due to differences in light-induced degradation and rating accuracy. These base case parameter values are assumed throughout the paper unless otherwise indicated. Error bars reflect uncertainties in efficiency and degradation, from Table 3. Bar tops assume low-end efficiencies (0.5% absolute below means) and high-end degradations (0.15%/yr above mean); bar bottoms reflect high-end efficiencies (0.5% absolute above means) and low-end degradations (0.15%/yr below mean). Monte carlo analysis requires additional uncertainty data.

parameter values used in Fig. 5 are assumed throughout the paper unless otherwise indicated. Fig. 6 shows the sensitivity of carbon intensity to previously analyzed continuous parameters, namely lifetime and degradation rate. An important non-continuous parameter is "production method". We find that, for Chinese mc-Si module production, using the "best technology" LCIs instead of the "mainstream" LCIs [37] produces a ~13% decrease in PV carbon intensity.

Like EOL processes, PV system lifetimes are highly uncertain because the large majority of installed PV capacity (97%) has been operating for under 10 years [7]. The 30 year lifetime assumed in most PV LCAs is based loosely on module warranties, not on physical limits. After 30 years, a PV system with typical 0.7% degradation per year will still be generating 78% of its day-one power output at small operating cost, and thus might not be voluntarily shut down by its owner. Given the large uncertainties in lifetime, Fig. 6 shows how PV carbon intensity varies over a range of lifetimes from 50% to 150% of the LCA-standard 30 years.

In contrast to lifetime uncertainty, uncertainties in rated efficiency, degradation, and weather can be approximately quantified based on empirical data, as shown by examples in Table 3. The numbers in Table 3 are meant to give approximate indicators of uncertainty and are not rigorous statistical measures. The last row follows NREL's recommendation to use weather data from multiple locations near the analyzed site to estimate uncertainties in energy production resulting from uncertainties in weather [42].

3.2. Temperature impacts

Inter-regional temperature variations can have a significant impact on the carbon intensity of PV power. As a case study, this paper analyzes two hypothetical identical open-ground mc-Si PV systems, one in the US northeast (Boston, Massachusetts) and one in the US southwest (Phoenix, Arizona). Using the equations in Tables S.1–S.3, cell temperature and module efficiency are calculated for a meteorologically average March day and plotted in Fig. 7.

Across all months, the generation-averaged cell temperature is 24.5 °C in Boston and 45.3 °C in Phoenix.[2] As a result, the modules' average year-one operating efficiency is 10% lower in Phoenix than in Boston (14.3% vs. 15.8%). Assuming operating efficiency and performance ratio independent of temperature, as is often done in PV LCA, would be equivalent to holding cell temperature constant at 25 °C or setting the thermal coefficient (γ) to 0%/°C in Table S.1. Doing so would negligibly change the estimated power output of the Boston system (< 0.1% change), but would overestimate the power of the Phoenix system by 11%, and thereby underestimate PV carbon intensity by 13% (31 vs. 35 gCO_2e/kWh).[3] Similar analyses can be applied to

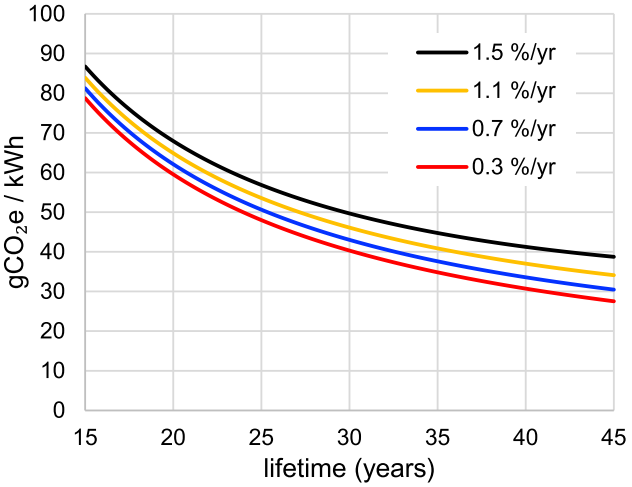

Fig. 6. Carbon intensity of PV power vs. lifetime at different degradation rates. Installation location is Sydney, Australia. Cell type is mc-Si. Rated module efficiency is 16%. Other parameters match base case values in Fig. 5.

[2] "Average" in this Section 3.2 means generation-averaged. Generation-averaged efficiency is the average efficiency at which electricity is generated. Time-averaged module efficiency is less relevant, because it weights night-time and cloudy-skies efficiency the same as day-time and clear-skies efficiency.

[3] Due to uncertainties described in Section 3.1, this paper reports carbon intensity to 2 significant figures. As a result, in a few cases, reported carbon intensities and reported percent difference might seem inconsistent, but are not. For example, if emissions for Scenarios A & B are computed as 19.3 & 20.7 gCO_2e/kWh, they are reported as 19 & 21 gCO_2e/kWh. To compute the percent difference, non-rounded numbers are always used in intermediate calculations. Thus, Scenario B emissions are computed to be 7% higher than Scenario A emissions, because (20.7–19.3)/19.3 = 0.07. If the rounded numbers were used for the intermediate calculation, the percent difference would be incorrectly computed as 11%, because (21–19)/19 = 0.11.

Table 3
Examples of uncertainty in parameters that impact the carbon intensity of PV power.

Variable	Typical uncertainty (corresponding ranges)	Based on:	Impact on PV carbon intensity: $\|(CI_{high} - CI_{low})\|/CI_{low} \times 100\%$
Rated efficiency of mc-Si modules purchased from a single product line and installed at a site	1% absolute (16–17%)	Specification sheets of 20 mc-Si product lines being sold by the top 3 Chinese module manufacturers in 2018 [43,44]. A single product line's specification sheet does not give a discrete rated efficiency, but rather a range, and for these 20 lines, that range is typically ~1% absolute	5%
Degradation rate of c-Si PV modules installed at a site	0.3%/yr (0.9–1.2%/yr)	The 95% confidence interval for measured degradation rates of 68c-Si modules tested at 5 sites in western India in the "hot & dry" climate category [30]. "Hot & dry" sites are defined in the survey as having ≥6 months with mean temperature over 30 °C and humidity under 55%, respectively. See Section 3.3 for more detail on this survey	10%
Lifetime avg. weather at a location	Irradiance in kWh/m^2/yr: Δ_{mean} ~ 47 (1000–1047, 2000–2047) Δ_{95} ~ 120 (1000–1120, 2000–2120) temperature: Δ_{mean} ~ 0.6 °C (10–10.6 °C, 20–20.6 °C) Δ_{95} ~ 1.5 °C (10–11.5 °C, 20–21.5 °C)	Irradiance and temperature differences across 30 pairs of locations, with each location-pair in the same US municipality. For example, 1 data-point is the recorded average irradiance difference between east & west Houston. Each location pair has a latitude difference under 0.2°. Data is from "TMY3" files in the National Solar Radiation Database [42]. Δ_{95} ~ 120 kWh/m^2/yr indicates that ~95% of these location-pairs have irradiance differences under 120 kWh/m^2/yr. Irradiance is GHI	2.5–4% for means 6–10% for 95-values

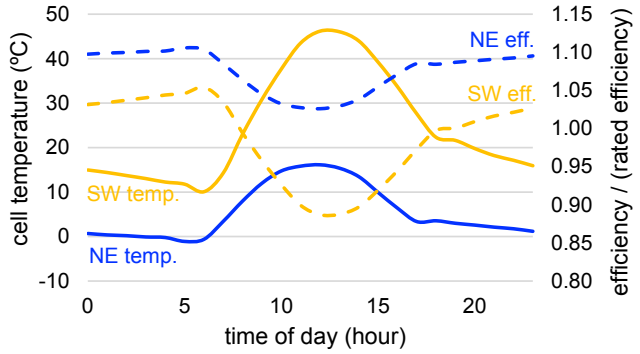

Fig. 7. Cell temperature (temp.) and operating efficiency (eff.) of mc-Si PV modules in the US northeast (NE, Boston) and the US southwest (SW, Phoenix) on an average March day, calculated using the PVWatts performance model outlined in Tables S.1–S.3. Averaging over the month smooths out hour-to-hour fluctuations. The weather data used are "Typical Meteorological Year" (TMY2) weather files used by PVWatts, with hourly data for 12 months. Each month is from a specific year, and which month comes from which year is determined by statistical methods to best represent a multi-year period. More information on TMY weather data can be found in [42].

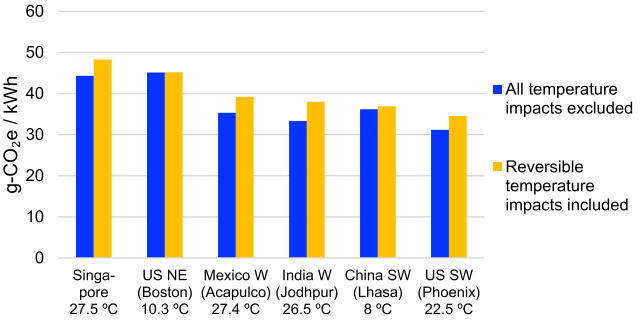

Fig. 8. Carbon intensity of mc-Si PV power in select regions. Mean ambient temperatures are at bottom. "Reversible temperature impacts included" (yellow) utilizes the full performance model outlined in methodology and the supplement. "All temperature impacts excluded" (blue) utilizes the same model, except with cell temperature held constant at 25 °C for all locations and times, and PR constant at 0.80, except for Boston which has PR of 0.79 due to snow losses). Note how excluding temperature impacts (blue) disturbs the monotonic decrease in carbon intensity left to right. Consistent with the base case, degradation of 0.7%/yr is assumed for all. Temperature-dependent degradation is discussed later.

other regions, as shown in Fig. 8. In each of the warm locations, neglecting reversible temperature impacts on module efficiency leads to underestimates of the carbon intensity of silicon PV power (by 9% in Singapore, 10% in the US southwest, 11% in western Mexico, and 13% in western India).

The analysis above addresses the denominator in carbon intensity, the kWh in gCO_2e/kWh, and can thus be applied to emissions of all pollutants, not only GHGs. This is one possible direction for future work and can help improve the understanding of PV power's environmental impacts and how they differ between regions.

Fig. 8 illustrates the reversible impacts of temperature on module efficiency. Irreversible impacts, i.e., temperature-induced degradation, can also be significant [30,31]. Modeling the complex modes of such impacts, including encapsulant discoloration, interconnect corrosion, and cell micro-cracking, is beyond the scope of this study. However, these effects can still be approximately accounted for based on empirical degradation rates. The 2014 and 2016 "All-India Surveys of PV Module Reliability" [31] found statistically significant differences in irreversible degradation between "hot" and "cold" climates of 0.96%/yr (1.18 vs. 0.24%/yr), based on 251 modules tested at 22 "hot" sites, and 126 modules tested at 5 "cold" sites. "Hot" sites had mean annual temperatures above 22 °C and were located in western, southern, and central India, while "cold" sites had temperatures below 12 °C and were located in northern India. This degradation difference means that the "hot" modules' power output typically declines by ~35% over 30 years, while the "cold" modules' output drops by ~12%. These numbers likely give a conservative estimate of the temperature-dependent degradation difference between climates because the survey excluded sites with mean degradation over 2%/yr, which filtered out 6 of 28 "hot" sites, but 0 of 5 "cold" sites.

As a case study of irreversible temperature effects on PV carbon intensity, we analyze two hypothetical mc-Si PV systems at two sites covered in the report, Chennai in southern India and Srinagar in northern India. Fig. 9 shows that accounting for temperature impacts significantly alters the inter-regional emissions comparison. If performance ratio is assumed constant between regions (blue bars), mc-Si PV power in northern India is estimated to be 21% more carbon intensive than in southern India (42 vs. 35 gCO_2e/kWh). If reversible

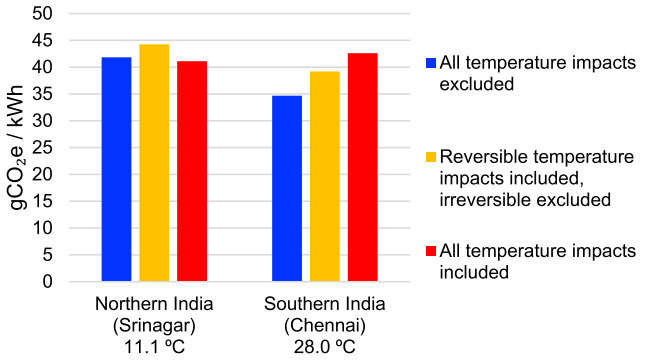

Fig. 9. Carbon intensity of PV power from mc-Si systems in northern and southern India. Mean ambient temperatures are at bottom. "All temperature impacts included" (red) utilizes the full performance model outlined in methodology and supplement, and empirically based degradation rates from [31] of 0.24 and 1.18%/yr in northern and southern India, respectively. "Reversible temperature impacts included, irreversible excluded" (yellow) utilizes the full model with variable temperature, and PV LCA-standard degradation of 0.7%/yr for both systems. "All temperature impacts excluded" (blue) utilizes the same model, except with cell temperature held constant at 25 °C and PV LCA-standard degradation of 0.7%/yr for both systems. Colors are consistent with Fig. 8.

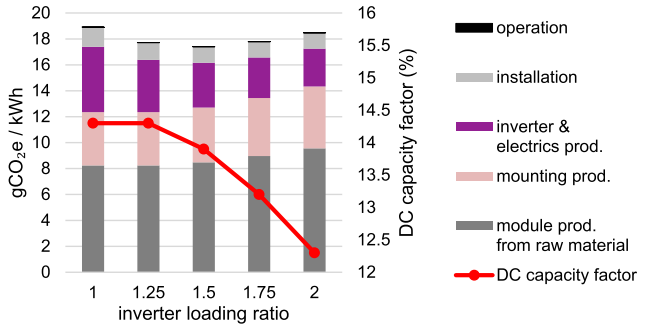

Fig. 10. Carbon intensity (left axis) & capacity factor (right axis) of CdTe PV systems with inverter loading ratios between 1 and 2. Installation location is near Charlotte, North Carolina, US, and installation type is roof-mounted with optimal tilt. Other parameters values match base case in Fig. 5. Carbon intensity drops as ILR rises from 1 to 1.5, due to reduced inverter material per module (see purple sections), and rises as ILR exceeds 1.5, due to reduced power output per module (see red line).

temperature effects are accounted for (yellow bars), the estimated gap shrinks to 13% (44 vs. 39 gCO_2e/kWh). And if all temperature effects are accounted for (red bars), it is estimated that mc-Si PV power in northern India is 5% *less* carbon intensive than in southern India (41 vs. 43 gCO_2e/kWh).

The locations in Figs. 8 and 9 are selected to demonstrate potential error in carbon intensity from ignoring temperature impacts. In some locations, this error will be negligible (e.g. in Boston the error is < 0.1%). However, it will not be negligible in warm locations or when comparing PV across regions with significant temperature differences (> 10 °C). Such temperature differences exist both between countries and within single large countries, including India, the US, and China. Given that emissions error from ignoring reversible temperature effects exceeds 10% in many warm regions, and that accounting for these effects is straightforward and requires negligible computational burden, as detailed in supplement 1, the authors recommend such accounting in future inter-regional PV emissions comparisons.

3.3. Inverter overloading

As commonly practiced (ILR < 1.5), inverter overloading slightly diminishes the carbon intensity of PV power. As a case study, this paper analyzes three hypothetical CdTe PV rooftop installations with ILRs of 1, 1.25, and 1.5, in the US state of North Carolina. These ILRs span the range seen generally in the US, and specifically at 40 CdTe projects operating in North Carolina in 2016, which had mean and maximum ILRs of 1.29 and 1.47, respectively [21]. The results are shown in Fig. 10. Increasing ILR from 1 to 1.5 reduces carbon intensity by 1.5 gCO_2e/kWh (8%). Overloading shrinks the inverter capacity required per module, thereby reducing GHG emissions from inverter production (see purple sections in Fig. 10). Thus, adding 50% more modules to an existing PV installation with ILR of 1 not only does not increase, but rather decreases the carbon intensity of power from that installation. This effect cannot be known *a priori* without doing the analysis, i.e., the finding of a small negative effect is itself notable. For silicon PV, the absolute change will be similar and the percent change smaller, due to silicon's greater module production emissions.

Increasing ILR further to 1.75[4] does not further reduce carbon intensity, due to "clipping". For a typical PV system with a self-limiting inverter, if its modules begin to generate DC power above the inverter's input capacity, the inverter "clips" the power by raising its voltage. Power that would be converted to AC if the inverter was bigger is instead never created. Clipping is rare for most PV systems without inverter overloading, because modules at real-world installations rarely reach their rated DC power. However, at high enough ILRs, power clipping becomes significant, as shown by the capacity factors (red line in Fig. 10) declining at ILRs above 1.25. This decline in carbon intensity's denominator (kilowatt-hours of power output) offsets the continued drop in inverter emissions, such that carbon intensity rises as ILR exceeds 1.5.

3.4. Horizontal 1-axis solar tracking

We find that in the US southwest, for mc-Si PV, horizontal 1-axis tracking reduces carbon intensity by 12% relative to the fixed-tilt base case (from 34 to 30 gCO_2e/kWh), consistent with previously published results [9]. Tracking produces this reduction despite requiring ~50% more structural metal (iron and aluminum) and ~30% more copper cable per module, compared to fixed-tilt mounting [26]. Emissions from producing the extra tracker materials (note the pink sections in Fig. 11) are offset by increased generation from tracking, such that overall carbon intensity decreases.

To determine if this ~10% emissions reduction holds for other regions and cell types, analogous calculations are applied to hypothetical mc-Si and CdTe PV systems at 10 other locations (the base cases from Fig. 5) and present them in Fig. 12, which underlines several related findings. (1) Location influences the emissions impact of tracking, via TEG; (2) tracking decreases the carbon intensity of mc-Si PV in most locations; (3) consistent with Sinha et al. [26], tracking reduces the carbon intensity of CdTe PV in the US southwest by ~3%; and (4) the US southwest is the exception to the rule: for most locations tested, tracking actually increases the carbon intensity of CdTe PV power. This includes many places with favorable economics for tracking and TEG above 13%. Near Sydney, Australia, for example, horizontal single-axis tracking increases both electricity output (by 14%) and carbon intensity (by 5%, from 19 to 20 gCO_2e/kWh). In Germany, where it is less common, tracking increases power output by 6% and emissions by 13% (from 31 to 35 gCO_2e/kWh).

The dependence on location is mainly driven by latitude and cloud cover. The greater the latitude, the greater the module tilt that maximizes incident irradiance, and the more irradiance is lost by

[4] ILRs of 1.7 or more are currently rare but not unseen, having been installed at large-scale PV projects (AC capacity > 1 MW) in at least 6 US states as of 2016 [21].

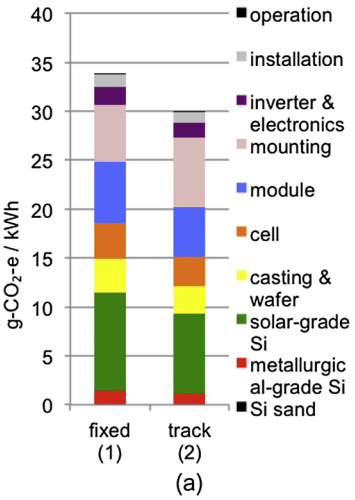

Input	Scenario 1	Scenario 2
Location of installation	US SW (Tuscon)	US SW (Tuscon)
Cell type	multi crystal Si	multi crystal Si
Installation type	utility, fixed tilt	utility, 1-axis tracking
Shading losses	2.5%	2.5%
Lifetime (yr)	30	30
Efficiency, initial STC rated	16.0%	16.0%
Degradation rate (/yr)	0.7%	0.7%
Inverter loading ratio	1	1
GHG emissions of electricity used to make panels (g-CO_2-e / kWh)	660	660
GHG emissions of electricity used to make BOS (g-CO_2-e / kWh)	500	500
Panel production typical of:	China	China
Shipping distance from panel production to installation (km)	21000	21000
Output	**Scenario 1**	**Scenario 2**
Life cycle GHG emissions (g-CO_2-e /kWh)	33.8	29.9
Capacity factor, lifetime avg, AC	18.4%	22.6%
Incident irradiance (kWh/m²/yr)	2295	2787

(b)

Fig. 11. (a) Carbon intensity of fixed-tilt vs. tracking PV in US SW. (b) Corresponding inputs to SoLCAT. To facilitate comparison with prior LCAs, ILR of 1 is used here, but it should be noted that ILR > 1 is now the norm for new installations, as discussed in Sections 1 and 3.3.

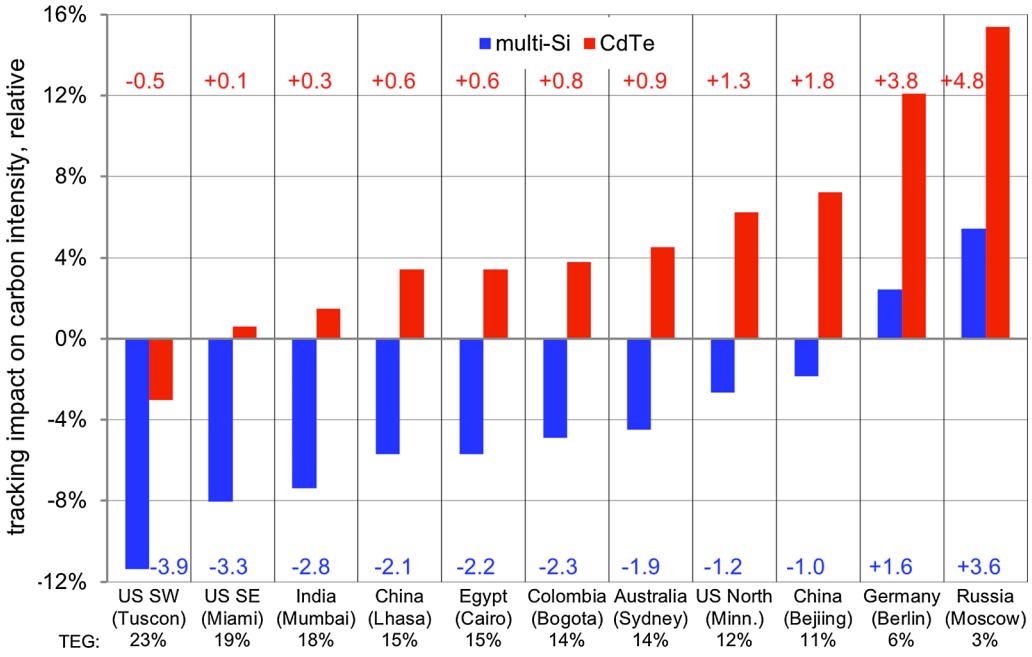

Fig. 12. The impact of horizontal 1-axis solar tracking on PV carbon intensity in different locations, for mc-Si PV (blue), and CdTe PV (red). The y-axis and bars indicate relative impact, i.e., percent change in carbon intensity compared to fixed PV at the same location: %-change = $(\boldsymbol{CI_{trackingPV}} - \boldsymbol{CI_{fixedPV}})/\boldsymbol{CI_{fixedPV}} \times 100\%$. The red and blue numbers indicate absolute impact (gCO_2e/kWh): absolute change = $(\boldsymbol{CI_{trackingPV}} - \boldsymbol{CI_{fixedPV}})$. Tracking energy gains (TEGs) are at bottom.

"reclining" to a horizontal tilt for 1-axis tracking.[5] Greater latitude also means more atmosphere for sunlight to travel through. This increases light scattering, as does greater cloud cover. The greater the fraction of ambient light that is scattered (i.e., diffuse), the less energy there is to be gained from tracking the sun's non-diffuse direct beam irradiance. Lower tracking energy gain (TEG) means less extra electricity over which to amortize extra emissions from tracker-production. For both module types, this explains why, as TEG decreases left to right in Fig. 12, tracking's emissions impact increases in relative terms (the bars).

The varying impact by module type can be explained with the following equations:

Let: $T \equiv$ the factor by which tracking increases electricity generation. E.g., If TEG = 20%, $T = 1.2$.
$e_{f,i} \equiv$ emissions of fixed PV system (gCO_2e). i = mc-Si or CdTe
$e_t \equiv$ emissions from adding tracking (gCO_2e)
$g_f \equiv$ generation from fixed PV system (kWh)
$g_t \equiv$ generation from tracking PV system (kWh)
$CI_f \equiv$ emissions per generation (carbon intensity) of fixed PV system (gCO_2e/kWh)
$CI_t \equiv$ emissions per generation (carbon intensity) of tracking PV system (gCO_2e/kWh)
$M \equiv$ factor by which tracking changes carbon intensity. Fig. 12 shows $(M - 1) \times 100\%$, the percent by which tracking changes carbon intensity.

[5] As described in Section 1, horizontal 1-axis tracking is the norm for large-scale tracking. Tilted 1-axis trackers do exist, but are much less common for reasons including self-shading issues and increased material demands and mechanical complexity to support and rotate tilted modules and to address wind effects.

Using these definitions:

$$M = CI_t/CI_f = [(e_{f,i} + e_t)/g_t]/[e_{f,i}/g_f] = [(e_{f,i} + e_t)/(T \times g_f)]/[e_{f,i}/g_f]M$$
$$= (e_{f,i} + e_t)/(T \times e_{f,i}) \quad (8)$$

Consider Eq. (8) when $e_{f,i} \gg e_t$, i.e., when emissions from module production are much larger than emissions from tracker production:

$$M_{flarge} = e_{f,i}/(T \times e_{f,i})$$
$$M_{flarge} = 1/T \quad (9)$$

M_{flarge} will always be less than 1, because T is always greater than 1. In other words, for a module type with large production emissions, adding tracking will reduce carbon intensity. This explains why adding tracking reduces the carbon intensity of mc-Si PV in most locations (blue bars in Fig. 12). Multi-Si module production is significantly more carbon intensive than CdTe module production, as seen in Fig. 2 and previously reported [37]. $e_{f,multi-Si}$ is approximately $11\times e_t$, whereas $e_{f,CdTe}$ is approximately $5 \times e_t$. Eq. (8) thus also explains why adding tracking increases CdTe PV's carbon intensity in most locations (red bars in Fig. 12):

$$M_{CdTe} = (e_{f,CdTe} + e_t)/(T \times e_{f,CdTe})$$
$$\cdots \approx (e_{f,CdTe} + e_{f,CdTe}/5)/(T \times e_{f,CdTe})$$
$$M_{CdTe} \approx 1.2/T \quad (10)$$

For M_{CdTe} to be less than 1, T must be greater than 1.2. In other words, CdTe PV requires TEG above 20% for tracking to reduce its carbon intensity, a TEG only possible in exceptionally sunny regions like the US southwest.

Fig. 13 illustrates the general principle behind both scenarios (high and low module emissions). In the future, if module production becomes more emissions-intensive relative to tracker production, tracking will more commonly decrease PV carbon intensity.

As with the temperature results, the analysis here can be generalized to other pollutants, not only GHGs. Eq. (8) is general to all emissions. Eq. (8) can also be generalized to all performance-affecting equipment, not only trackers:

$$M^\circ = (e_{f,i}^\circ + e_t^\circ)/(T^\circ \times e_{f,i}^\circ) \quad (11)$$

where M° is the factor by which the equipment changes emissions intensity ($g_{pollutant}$/kWh), T° is the factor by which the equipment changes power output, $e_{f,i}^\circ$ is emissions (e.g., GHGs or any other pollutant) from the generator before adding the equipment ($g_{pollutant}$), and e_t° is the emissions from the added equipment ($g_{pollutant}$). For example, lithium ion batteries coupled with PV can be analyzed as performance-affecting equipment with T° typically equal to 0.8–0.95 [45]. Future work should explore applying these equations to other pollutants and other PV-coupled equipment including batteries.

Given that one motivation for incorporating PV performance modeling into PV LCA is to better model solar tracking, it is relevant to note that three of the prior LCAs addressing tracking assume unrealistic TEGs. Bayod-Rújula et al. [22] accurately estimate 2-axis TEG in central Spain of 38%, but then generalize this number to Berlin, where in reality TEG will be at least 35% lower, due to greater latitude and diffuse light fraction. Beylot et al. [23] assume an exceptionally low TEG of 5% for 1-axis tracking with 30° tilt, given annual irradiance of 1700 kWh/m^2/yr on a 30°-tilted plane, at a hypothetical project of unspecified location. Desideri et al. [24] assume a ~5-times-greater TEG of 26%, also for 1-axis tracking with 30° tilt (1928 vs. 1530 kWh)), given direct normal irradiance of 1600–1800 kWh/m^2/yr at a hypothetical project near Gela, Sicily. For the conditions stated in [24], 26% TEG is significantly higher than the 20% TEG that PVWatts and Eq. (7) would estimate in Gela. This may be due to the study's use of an AC power equation that assumes irradiance on a surface that is normal to the sun's rays; however, 1-axis tracking cannot keep a module surface normal to sunlight, unlike 2-axis tracking. Using PVWatts and Eq. (7) to estimate TEG for a 2-axis tracking system in Gela gives a value of 25%, relative to a fixed PV system facing south with 30° tilt.

3.5. Manufacturing location

A harmonization series provides insight into emissions differences between Chinese and European supply chains for mc-Si modules. Consider two scenarios in which mc-Si modules are installed at a utility PV site near Berlin, Germany. The hypothetical German installer has a choice of modules. In scenario 1 the modules are sourced from China; in scenario 2, from Germany. Inputs to SoLCAT are selected accordingly for production inventory, production grid emissions, and shipping distance from production to installation, as seen in Fig. 14. Production grid emissions are based on 2015 IEA data on electricity emissions (470 and 660 gCO_2e/kWh for Germany and China, respectively) [40], and shipping distance is based on the commercial ports nearest to production (Shanghai) and installation (Bremerhaven) [46].

Under these conditions, the life cycle GHG emissions of the Chinese-produced modules are 27% higher (68 vs. 53 gCO_2e/kWh) than German-produced modules. To explain this emissions gap, we utilize step-by-step harmonization. First we harmonize shipping distance to 17300 km in both scenarios, and second we harmonize GHG emissions of upstream electricity to 660 gCO_2e/kWh in both scenarios. Fig. 15(a) shows that (1) shipping contributions to the emissions difference are small (only 7% of the initial gap), and (2) electricity source determines

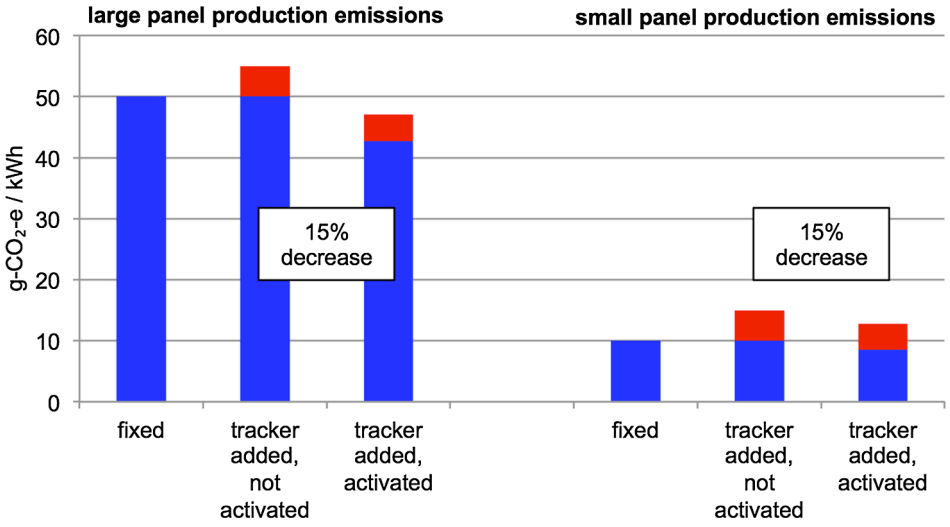

Fig. 13. Illustration of how panel production emissions influence whether tracking decreases (left) or increases (right) carbon intensity, relative to fixed PV. Left and right systems have the same location and power output per panel. Activating tracking on both boosts power by 17%, a typical TEG for a sunny location. Red is the tracker contribution to emissions. In terms of Eq. (8) definitions, red represents e_t/g_f in the "not activated" bars, and e_t/g_t in the "activated" bars. Emissions values in this figure are arbitrary and chosen to illustrate the concept. TEG of 17% is assumed, giving a 15% reduction in carbon intensity upon activation.

Input	Scenario 1	Scenario 2
Location of installation	Germany (Berlin)	Germany (Berlin)
Cell type	multi crystal Si	multi crystal Si
Installation type	utility, fixed tilt	utility, fixed tilt
Shading losses	2.5%	2.5%
Lifetime (yr)	30	30
Efficiency, STC rated	16.0%	16.0%
Degradation rate (/yr)	0.7%	0.7%
Inverter loading ratio	1	1
GHG emissions of electricity used to make panels (g-CO_2-e / kWh)	660	470
GHG emissions of electricity used to make BOS (g-CO_2-e / kWh)	470	470
Panel prod. typical of:	China	Europe
Shipping distance from panel production to installation (km)	17300	300
Output, lifetime average	**Scenario 1**	**Scenario 2**
Life cycle GHG emissions (g-CO_2-e /kWh)	67.5	53.2
Capacity factor, DC	9.2%	9.2%
Incident irradiance (kWh/m²/yr)	1071	1071

Fig. 14. GHG emissions (red box) of mc-Si PV installed in Germany and produced in China or Europe, and corresponding inputs to SoLCAT (differences in yellow box).

a large part of the emissions difference (48%), consistent with previous LCAs [9,28]. That is, Chinese module production relies on grid electricity that is more carbon-intensive than European electricity. However, as the final harmonization shows, a nontrivial emissions gap remains, approximately half the original difference. In other words, even with identical shipping distances and electricity sources, the two regions' module supply chains are non-identical in emissions-relevant ways. Fig. 15(b) shows how: Chinese module production not only uses electricity that is more carbon-intensive (more GHGs per input kWh); it also uses a greater *amount* of that electricity (more input kWh per module), and in addition, more fuel. The mainstream Chinese and European LCIs [37] indicate that, across all module production stages (silica sand acquisition through module assembly in Fig. 2), Chinese module production uses ~30% more electricity per module manufactured.

4. Conclusion

This paper first quantifies the impacts of previously explored variables on the carbon intensity of photovoltaic power, including

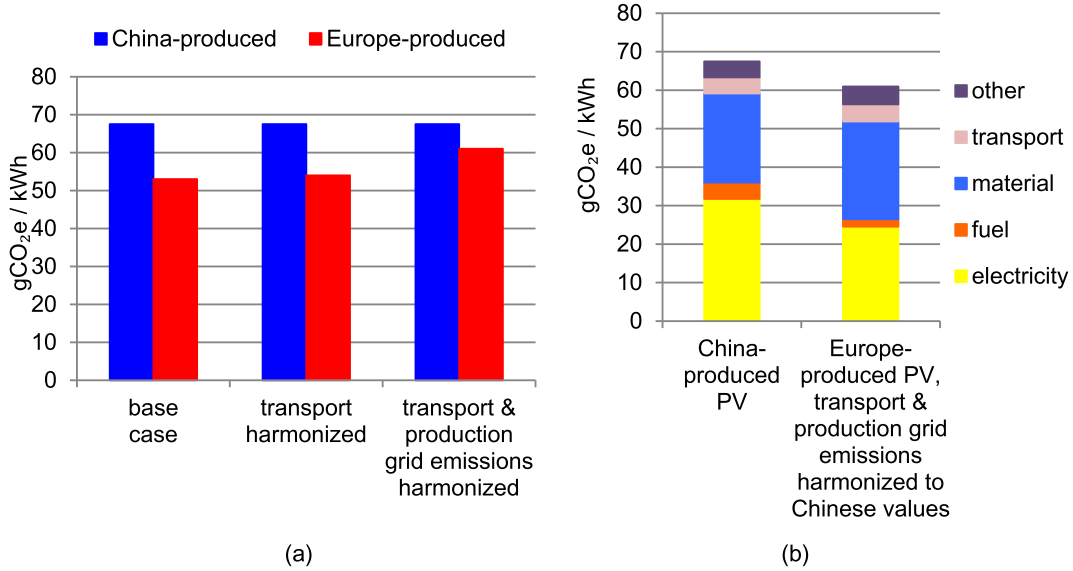

Fig. 15. (a) Impact of harmonization on GHG emissions of mc-Si PV. Transport is harmonized by setting European panel shipping distance equal to Chinese value of 17300 km. Grid emissions are harmonized by setting European grid emissions equal to Chinese value of 660 gCO_2e/kWh. (b) Emissions breakdown by category of input to foreground stages. Foreground refers to the life cycle stages in Fig. 2. Note: foreground gives an approximate sense of stages controlled by companies in the PV supply chain. "Material" "transport" and "other" GHG emissions in the foreground can ultimately be traced back to carbon fuel use in the background (e.g. in steel production) in most cases.

irradiance, rated module efficiency, lifetime, and degradation. We then find that, compared to the impacts of these variables, (1) emissions impacts from temperature effects are significant in warm regions (order 10% increase), (2) emissions differences between Chinese and European photovoltaic manufacturing are significant (~25% difference), (3) emissions impacts from adding solar tracking are significant in some places (up to ± 12% change) and negligible in others (± 1%), and (4) impacts from inverter overloading are small (less than 2 gCO_2e/kWh decrease). The analysis of overloading, tracking, and temperature effects demonstrates the benefit to photovoltaic life cycle assessment of incorporating more detailed models of photovoltaic performance. Potential improvements in our model include incorporation of end-of-life emissions, future foreground life cycle inventories, other photovoltaic technologies (e.g., bifacial modules), and transmission from generation-site to end-use site. Potential directions for future research include: exploration of why Chinese production of silicon photovoltaic panels uses significantly more electricity than European production; application of the temperature models described to other pollutants, not only GHGs; and application of the tracking equations described to other pollutants and other equipment, such as batteries.

Finally, it should be noted that in many cases the largest greenhouse gas emissions impact of a photovoltaic system derives not from incident irradiance or cell type or use of tracking or any other system feature, but rather from displacement of competing power sources. The most carbon intensive mainstream solar power (typical rooftop single-crystalline silicon photovoltaics installed in northern Europe) emits less than one fourth the life cycle greenhouse gas emissions of the least carbon intensive mainstream fossil power (natural gas combined cycle), if attributional life cycle assessment is used for the analysis, as in this paper. Rigorously analyzing such emissions displacements requires the method of consequential life cycle assessment, as opposed to process-based life cycle assessment. Consequential life cycle assessment is also needed to analyze the emissions impacts of measures, such as grid-level energy storage, that aim to make photovoltaic power as dispatchable as power from other generation technologies.

Acknowledgements

The authors would like to thank: Dr. Mark Disko and Dr. Heather Elsen from ExxonMobil Research and Engineering for their inputs; and Professor Robert C. Armstrong for his support and discussion. This research was supported by ExxonMobil Research and Engineering. Patrick Brown was supported by the US Department of Energy (DOE) Office of Energy Efficiency and Renewable Energy (EERE) Postdoctoral Research Award through the EERE Solar Energy Technologies Office under DOE contract number DE-SC00014664.

Declaration of interest

None.

Appendix A. Supplementary material

Supplementary data to this article can be found online at https://doi.org/10.1016/j.apenergy.2019.01.012.

References

[1] IEA. Energy, climate change & environment. Paris (France): OECD Publishing; 2016.
[2] The Energy Initiative MIT. The future of solar energy. MIT; 2015. p. 127.
[3] REN21. Renewables 2018 global status report; 2018. p. 90.
[4] GlobalData. Solar PV generation statistics. < https://power-globaldata-com.libproxy.mit.edu/capacityandgeneration.aspx?type=SolarPV > [accessed 1 December 2017].
[5] ExxonMobil. 2017 Outlook for energy: a view to 2040; 2017. p. 26.
[6] BNEF. Bloomberg new energy finance report 2017. Bnef 2017;1–60.
[7] Fraunhofer Institute for Solar Energy. Photovoltaics report; 2017. p. 4.
[8] California Energy Commission. Total system electric generation. < http://www.energy.ca.gov/almanac/electricity_data/total_system_power.html > [accessed 1 December 2017].
[9] Leccisi E, Raugei M, Fthenakis V. The energy and environmental performance of ground-mounted photovoltaic systems - a timely update. Energies 2016;9. https://doi.org/10.3390/en9080622.
[10] Arvesen A, Hertwich EG. Assessing the life cycle environmental impacts of wind power: a review of present knowledge and research needs. Renew Sustain Energy Rev 2012;16:5994–6006.
[11] Skone TJ. NETL. Power generation technology comparison from a life cycle perspective. Pittsburgh, PA; 2013.
[12] ISO. Environmental management—life cycle assessment—requirements and guidelines; 2006.
[13] Hou G, Sun H, Jiang Z, Pan Z, Wang Y, Zhang X, et al. Life cycle assessment of grid-connected photovoltaic power generation from crystalline silicon solar modules in China. Appl Energy 2016. https://doi.org/10.1016/j.apenergy.2015.11.023.
[14] Akinyele DO, Rayudu RK, Nair NKC. Life cycle impact assessment of photovoltaic power generation from crystalline silicon-based solar modules in Nigeria. Renew Energy 2017;101:537–49. https://doi.org/10.1016/j.renene.2016.09.017.
[15] Kabakian V, McManus MC, Harajli H. Attributional life cycle assessment of mounted 1.8 kWp monocrystalline photovoltaic system with batteries and comparison with fossil energy production system. Appl Energy 2015. https://doi.org/10.1016/j.apenergy.2015.04.125.
[16] Yu Z, Ma W, Xie K, Lv G, Chen Z, Wu J, et al. Life cycle assessment of grid-connected power generation from metallurgical route multi-crystalline silicon photovoltaic system in China. Appl Energy 2017. https://doi.org/10.1016/j.apenergy.2016.10.051.
[17] Hsu DD, O'Donoughue P, Fthenakis V, Heath GA, Kim HC, Sawyer P, et al. Life cycle greenhouse gas emissions of crystalline silicon photovoltaic electricity generation: systematic review and harmonization. J Ind Ecol 2012;16.
[18] Peng J, Lu L, Yang H. Review on life cycle assessment of energy payback and greenhouse gas emission of solar photovoltaic systems. Renew Sustain Energy Rev 2013;19:255–74.
[19] Frischknecht R, Heath G, Raugei M, Sinha P, de Wild-Scholten M, Fthenakis V, et al. Methodology guidelines on life cycle assessment of photovoltaic electricity, 3rd ed. IEA PVPS Task 12 Int Energy Agency Photovolt Power Syst Progr; 2016.
[20] Dobos AP. PVWatts Version 5 Manual (NREL/TP-6A20-62641); 2014.
[21] EIA. Form EIA-860 : annual electric generator report; 2016.
[22] Bayod-Rújula ÁA, Lorente-Lafuente AM, Cirez-Oto F. Environmental assessment of grid connected photovoltaic plants with 2-axis tracking versus fixed modules systems. Energy 2011;36:3148–58.
[23] Beylot A, Payet JÔ, Puech C, Adra N, Jacquin P, Blanc I, et al. Environmental impacts of large-scale grid-connected ground-mounted PV installations. Renew Energy 2014;61:2–6.
[24] Desideri U, Zepparelli F, Morettini V, Garroni E. Comparative analysis of concentrating solar power and photovoltaic technologies: technical and environmental evaluations. Appl Energy 2013;102:765–84.
[25] Bolinger M, Seel J, LaCommare KH. Utility-scale solar 2016. Lawrence Berkeley Natl Lab; 2017.
[26] Sinha P, Schneider M, Dailey S, Jepson C, De Wild-Scholten M. Eco-efficiency of CdTe photovoltaics with tracking systems. In: Conference record of the 39th IEEE photovoltaic specialists conference (PVSC), Tampa, FL, USA; 2013. p. 3374–8.
[27] Perpiñan O, Lorenzo E, Castro MA, Eyras R. Energy payback time of grid connected PV systems: comparison between tracking and fixed systems. Prog Photovoltaics Res Appl 2009;17:137–47.
[28] Nian V. Impacts of changing design considerations on the life cycle carbon emissions of solar photovoltaic systems. Appl Energy 2016;183:1471–87.
[29] Sandia National Laboratories. PV performance modeling collaborative (PVPMC) website; 2017. < https://pvpmc.sandia.gov > [accessed 1 December 2017].
[30] Jordan DC, Kurtz SR, VanSant K, Newmiller J. Compendium of photovoltaic degradation rates. Prog Photovoltaics Res Appl 2016;24:978–89. https://doi.org/10.1002/pip.2744.
[31] Chattopadhyay S, Dubey R, Kuthanazhi V, Zachariah S, Bhaduri S, Mahapatra C, et al. All-India survey of photovoltaic module reliability: 2016. Mumbai, India; 2017.
[32] Wernet G, Bauer C, Steubing B, Reinhard J, Moreno-Ruiz E, Weidema B. The ecoinvent database version 3 (Part I): overview and methodology. Int J Life Cycle Assessment 2016;21(9):1218–30http://link.springer.com/10.1007/s11367-016-1087-8.
[33] Gagnon P, Margolis R, Melius J, Phillips C, Elmore R. Rooftop solar photovolatic technical potential in the united states: a detailed assessment. NREL; 2016. p. 82. < https://www.nrel.gov/docs/fy16osti/65298.pdf > .
[34] Jean J, Brown PR, Jaffe RL, Buonassisi T, Bulović V. Pathways for solar photovoltaics. Energy Environ Sci 2015;8:1200–19. https://doi.org/10.1039/c4ee04073b.
[35] Jungbluth N, Stucki M, Flury K, Frischknecht R, Busser S. Life cycle inventories of photovoltaics. Uster, CH: ESU-Services Ltd.; 2012.
[36] Gençer E, Miskin C, Sun X, Khan MR, Bermel P, Alam MA, et al. Directing solar photons to sustainably meet food, energy, and water needs. Sci Rep 2017;7. https://doi.org/10.1038/s41598-017-03437-x.
[37] Frischknecht R, Itten R, Sinha P, de Wild-Scholten M, Zhang J, Fthenakis V. Life cycle inventories and life cycle assessment of photovoltaic systems; Report IEA-PVPS T12-04:2015. Paris (France): International Energy Agency (IEA); 2015.

[38] Allen MR, Barros VR, Broome J, Cramer W, Christ R, Church JA, et al. IPCC fifth assessment synthesis report-climate change 2014 synthesis report; 2014.
[39] de Wild-Scholten M. Life cycle assessment of photovoltaics status 2011, Part 1 data collection. Groet (Netherlands): SmartGreenScans; 2014.
[40] IEA. CO_2 emissions from fuel combustion. Paris (France): OECD Publishing; 2017. p. 2017.
[41] Gilman P, Dobos A, DiOrio N, Freeman J, Janzou S, Ryberg D. SAM photovoltaic model technical reference update; 2018.
[42] US National Renewable Energy Laboratory. System advisor model website; 2018. < https://sam.nrel.gov/weather > [accessed 1 March 2018].
[43] Jinko Solar. Download center poly-module datasheets; 2018. < https://www.jinkosolar.com/download_356.html > [accessed 1 February 2018].
[44] Trina Solar. Products & solutions downloads: multicrystalline datasheets; 2018. < http://trinasolar.com > [accessed 1 February 2018].
[45] Mitavachan H. Comparative life cycle assessment of stationary battery storage technologies for balancing fluctuations of renewable energy sources. Thesis; 2014.
[46] Sea-distances. Port distances calculator; 2017. < https://sea-distances.org > [accessed 1 December 2017].